chemosensors

MDPI

Article

Macrocyclic Compounds Comprising Tris(3-Aminopropyl)Amine Units and Fluorophore Moieties: Synthesis and Spectroscopic Studies in the Presence of Metal Salts

Daria S. Kuliukhina, Nataliya M. Chernichenko, Alexei D. Averin *, Anton S. Abel, Olga A. Maloshitskaya and Irina P. Beletskaya

Department of Chemistry, Lomonosov Moscow State University, Moscow 119991, Russia
* Correspondence: alexaveron@yandex.ru; Tel.: +7-495-939-11-39

Abstract: The synthesis of a variety of polyazamacrocyclic compounds comprising structural units of tris(3-aminopropyl)amine (TRPN) and oxadiamines, decorated with one or two fluorophore groups (dansyl or quinoline) at different nitrogen atoms, was carried out using Pd(0)-catalyzed amination. The dependence of the yields of the macrocycles on the synthetic path was observed. The spectrophotometric and fluorescent properties of the target compounds were studied, and their coordination with metal cations using UV–vis, fluorescence spectra as well as NMR titration was investigated. The stoichiometry and binding constants of several complexes with Cu(II), Zn(II), Cd(II), Pb(II) and Hg(II) were established. Three of the six studied macrocycles can be judged as prospective detectors of Zn(II) cations due to the substantial enhancement of fluorescence.

Keywords: tris(3-aminopropyl)amine; macrocycles; palladium catalysis; amination; fluorescence; detection

check for updates

Citation: Kuliukhina, D.S.; Chernichenko, N.M.; Averin, A.D.; Abel, A.S.; Maloshitskaya, O.A.; Beletskaya, I.P. Macrocyclic Compounds Comprising Tris(3-Aminopropyl)Amine Units and Fluorophore Moieties: Synthesis and Spectroscopic Studies in the Presence of Metal Salts. *Chemosensors* **2023**, *11*, 186. https://doi.org/10.3390/chemosensors11030186

Academic Editors: Guo-Hui Pan, Hongshang Peng and Biao Dong

Received: 1 February 2023
Revised: 4 March 2023
Accepted: 7 March 2023
Published: 10 March 2023

1. Introduction

Tetrapodal tetraaza ligands formed on the basis of tris(2-aminoethyl)amine (TREN) and tris(3-aminopropyl)amine (TRPN) attract the interest of the researchers, as they can play a role in the construction of various functional molecules and materials, e.g., macrocyclic and cryptand compounds comprising such structural units can be used for the molecular recognition of cations, anions and small organic molecules [1–4]; thus, the strategies for the construction of such compounds attract researchers [5]. Thus, a macrocycle with two TREN moieties and two 2,6-disubstituted pyridines decorated with two 1-naphthyl fluorophores connected by aminomethyl linkers was studied for the complexation with Cu(II) and Zn(II) [6] as well its analog with 4-quinolinyl fluorophores [7]. Several TREN derivatives were reported as efficient chelators of lanthanide ions [8]. TREN was also used for the end-capping of the hemicryptophane molecule comprising numerous polyoxysubstituted phenyl fragments. The compound is water-soluble, and its complex with Gd(III) is used as contrast agent in MRT [9]. A review on the manganese complexes with branched polyaza ligands (macrocyclic and open-chain) has been published recently [10].

TRPN is far less studied than TREN, and the majority of its derivatives do not contain macrocyclic moieties. Depending on the nature of the substituents at the nitrogen atoms, metal complexes of various structures and with different applications were obtained [11–14]. Enough simple acyclic receptors on the basis of urea and thiourea were synthesized from TRPN and studied in binding inorganic anions [15]. Some derivatives of this branched amine were investigated as antimalarial agents, e.g., tris(quinoxaline) [16] and tris(phenanthroline) [17] derivatives of TRPN showed antiparasitic activity. Other tripodal receptors were synthesized using 4-nitrophenyl isothiocyanate, 4-nitrophenylsulphonyl

chloride and 4-nitrophenylbenzoyl chloride [18]. Such ligands demonstrate good selectivity towards cyanide anions. *N*-substituted derivatives of TRPN and their complexes were reported for the recognition of the azide-anion [19,20]. More sophisticated complex structures with TRPM structural fragments were reported for sensing *N*-Acetyl-β-d-glucosaminidase [21]. There are some examples of the use of TRPN derivatives as building blocks for the construction of MOFs [22]. Functional materials on the basis of TRPN are prospective for CO_2 binding [23,24]. Complexes of cyclic and bicyclic ligands with transition metals containing TRPN moieties find application as catalysts [25], and they can also bind with DNA [26]. Quite rare are examples where TRPN was used for the construction of macrocyclic systems. Cryptands synthesized by the reaction of TRPN with trialdehyde [27] or 2,5-furandialdehydes have been reported [28]. A macrocycle on the basis of 1,8-disubstituted anthracene with TRPN was studied for the detection of Hg(II) and Cu(II) using fluorescent spectroscopy [29].

In the present work, we propose a convenient synthetic route to polyazamacrocycles comprising structural fragments of tris(3-aminopropyl)amine (TRPN) and oxadiamines bearing fluorophore groups at different nitrogen atoms (endocyclic and exocyclic). Previously, we accumulated substantial experience in the synthesis of various *N*- and *O*-containing macrocycles [30] and polymacrocycles [31], including those with fluorophore groups as well as chiral moieties [32], and demonstrated the wide possibilities of Pd(0)-catalyzed amination for this purpose. The main peculiarity of the proposed TRPN-derived macrocycles is the presence of the exocyclic 3-aminopropyl substituent and the possibility of varying the position of the fluorophore group (such as 5-(dimethylamino)naphthalene-1-sulfonyl (dansyl), 6- or 3-quinolinyl) by attaching it to either the endocyclic or exocyclic nitrogen atom. Special attention is paid to the investigation of the coordination of metal cations and the possibilities of using these macrocycles for spectrophotometric and fluorescent detection.

2. Materials and Methods

^{1}H and ^{13}C NMR spectra were recorded with a Bruker Avance-400 spectrometer in $CDCl_3$, and residual peaks of the solvent were as used as standards (δ 7.26 ppm and 77.0 ppm, respectively). UV–vis spectra were recorded with an Agilent Cary 60 spectrophotometer, and the spectra of fluorescence were obtained with a Hitachi F2700 spectrofluorometer using acetonitrile UHPLC grade (Fluka). MALDI-TOF mass spectra were obtained with a Bruker Autoflex II spectrometer with dithranol as the matrix and (polyethylene) glycols as the internal standards. Tris(3-aminopropyl)amine (**1**), dioxadiamine **12**, 5-(dimethylamino)naphthalene-1-sulfonyl chloride (dansyl chloride), 6-bromoquinoline, 3-bromoquinoline and the phosphine ligands *rac*-BINAP, DavePhos, *t*BuDavePhos, *t*BuONa and K_2CO_3, were purchased from Sigma-Aldrich Co and ACBR Co and used without special purification. Column chromatography was performed using silica gel 40–63 μm from Macherey-Nagel Co, 1,4-dioxane was purified by distillation over sodium under argon, acetonitrile for the syntheses was distilled over CaH_2 and dichloromethane and methanol were freshly distilled prior to use. $Pd(dba)_2$ was synthesized using a known procedure [33], and *N*,*N*′-di(3-bromophenyl)-substituted dioxadiamine **6** and *N*,*N*′-di(3-bromophenyl)-substituted trioxadiamine **17** were obtained by a described method [34]. A description of the syntheses of compounds **2**–**5**, **7**–**11**, **13**–**16** and **18**–**25** and their spectral data are given in the Supplementary Materials.

An investigation of the ability of the macrocycles **7**, **8**, **16**, **22**, **23** and **25** to detect metal cations by means of UV–vis and fluorescent spectroscopies was carried out as follows. The spectrofluorimetric quartz cuvette (l = 1 cm) was charged with 3 mL of the solution of the corresponding ligand in MeCN (UHPLC grade) with the following concentrations: 4.8 μM (**7**), 23.0 μM (**8**), 17.5 μM (**16**), 14.3 μM (**22**), 21.2 μM (**23**) and 12.3 μM (**25**). Solutions of each of the metal perchlorates (Li(I), Na(I), K(I), Mg(II), Ca(II), Ba(II), Al(III), Cr(III), Mn(II), Fe(II), Co(II), Ni(II), Cu(II), Zn(II), Cd(II), Hg(II), Pb(II) and Ag(I)) or the nitrates (Ga(III), In(III) and Y(III)) in MeCN (UHPLC grade) with concentrations of 0.01 M were

added with a Hamilton syringe directly to the spectrofluorimetric cuvette successively (to make 1, 2, 3, 5 and 10 equiv. of each metal); UV–vis and fluorescence spectra were registered after each addition. Spectrophotometric and spectrofluorimetric titrations were carried out by adding metal perchlorates in increments of 0.05 equiv. with the following concentrations of the ligands: 318 μM (**16**, UV–vis titration), 191 μM (**22**, UV–vis titration), 39 μM (**22**, spectrofluorimetric titration), 252 μM (**23**, UV–vis titration), 160 μM (**25**, UV–vis titration). Stability constants were calculated using nonlinear least squares analysis by means of HYPERQUAD software after the factor analysis of the combined datasets [35]. NMR titrations were carried out by adding metal perchlorates (C = 0.2 M in CD_3CN) in increments of 0.1 equiv. to the solutions of the corresponding macrocycles in CD_3CN with the following concentrations of the ligands: 0.041 M (**16**), 0.036 M (**22**) and 0.046 M (**25**). The compositions of the complexes and binding constants were calculated using the EQNMR [36] and BindFit [37] programs.

3. Results and Discussion

3.1. Synthesis of the Macrocycles Comprising a Sructural Unit of Tris(3-Aminopropyl)Amine

The main idea of the synthetic approach to the fluorescent macrocyclic compounds comprising endocyclic tris(3-aminopropyl)amine fragments was the combination of this unit with the oxadiamine structural units via 1,3-phenylene linkers and the introduction of fluorophore groups such as dansyl (5-dimethylaminonaphthalene-1-sulfonyl) and quinoline to nitrogen atoms of the macrocycles at various positions. The extensive application of the Buchwald–Hartwig amination reaction for constructing C-N bonds is characteristic of this approach. At first, we attempted the synthesis of the macrocycles bearing fluorophore groups at the exocyclic nitrogen atom of the 3-aminopropyl group (Scheme 1). For this purpose, *N*-dansyl and *N*-quinolin-6-yl-substituted tris(3-aminopropyl)amines **2** and **4** were synthesized from free tris(3-aminopropyl)amine (**1**) (Scheme 1). The reaction with dansyl chloride was carried out by a very slow addition of the reagent to an excess of the tetraamine taken as a dilute (0.065 M) solution in MeCN. The yield of the target monodansyl derivative **2** was 50%, while the side product—the didansylated tetraamine **3**—was isolated in 25% yield. The heteroarylation of **1** with 6-bromoquinoline was conducted using a universal catalytic system $Pd(dba)_2$/BINAP (8/9 mol%) (dba = dibenzylidene acetone, BINAP = *rac*-2,2′-diphenylphoshino-1,1′-binaphthalene) in dioxane in the presence of *t*BuONa as a base. The application of a twofold excess of **1** in this case was also important to promoting the formation of the monoquinolinyl-substituted product **4** (48% yield), though the diquinolinyl derivative **5** was also obtained (24% yield). The attempt to apply the diminished amount of the catalyst (4/4.5 mol%) failed, as the conversion of 6-bromoquinoline reached only 50%.

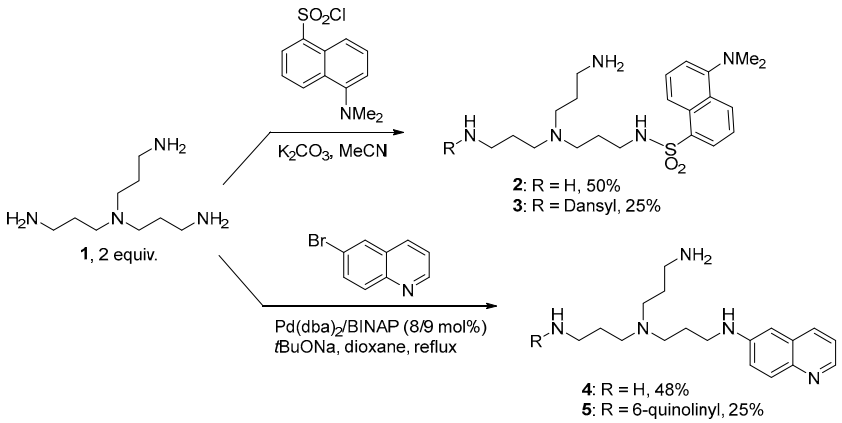

Scheme 1. The synthesis of dansyl- and 6-quinolinyl-substituted tris(3-aminopropyl)amine 2 and 4.

To afford the desired macrocycles, the reactions of macrocyclization were carried out between dansyl or quinolinyl derivatives (**2** or **4**) and *N*,*N*′-di(3-bromophenyl)-substituted dioxadiamine **6**, which was prepared from the free dioxadiamine in accordance with the

previously described method [34] (Scheme 2). The reactions were run in the presence of $Pd(dba)_2$/*t*BuDavePhos (16/18 mol%) (*t*BuDavePhos = 2-(di*tert*-butylphosphino)-2′-dimethylaminobiphenyl). This ligand, like its analog DavePhos, promotes the diamination of aryl halides and is efficient, especially under dilute conditions (in the macrocyclization reactions, we employ 0.02 M solutions of the reagents in dioxane). It was found that the reaction of **6** with the dansyl derivative **2** was inefficient, and the desired macrocycle **7** could not be isolated; however, the reaction with the quinolinyl derivative **4** was successful, and the yield of the corresponding macrocycle **8** was 38%.

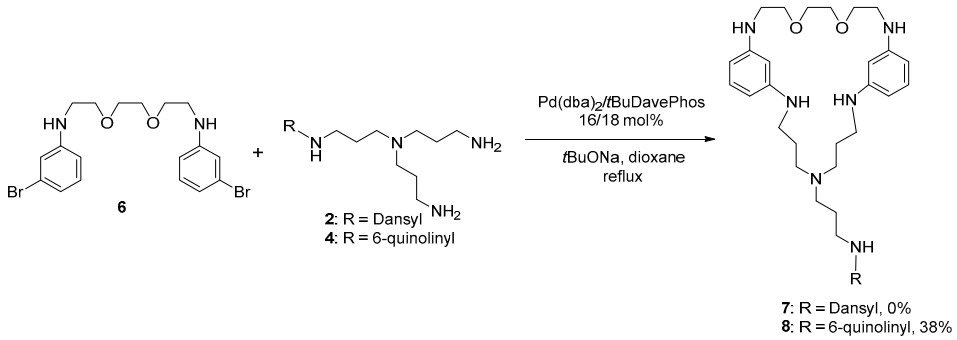

Scheme 2. Synthesis of 6-quinolinyl-substituted macrocycle 8.

The alternative route to the macrocycle **7** used a three-step procedure. At first, branched tetraamine **1** was converted into its *N*,*N*′-di(3-bromophenyl) derivative **9** by the reaction with two equiv. of 1,3-dibromobenzene (Scheme 3). The main side product in this process was the triarylated compound **10**, which was isolated in a comparable yield; however, attempts to increase the yield of the target compound **9** and to hamper the formation of **10** by varying the stoichiometry of the process and the catalyst loading did not improve the result. The slow reaction of compound **9** with strictly one equiv. of dansyl chloride in $MeCN/CH_2Cl_2$ (10:1) helped to avoid the formation of various polydansylated derivatives, and monodansyl compound **11** was obtained in 67% yield. At the last step, macrocyclization with a free dioxadiamine **12** (1.5 equiv.) gave rise to the target macrocycle **7** in a 23% yield. Here, the use of 1.5-fold excess of the diamines in the macrocyclization reactions was shown to slightly increase the yields of the desired products. The attempt to synthesize compound **11** by an alternative procedure, using the Pd-catalyzed arylation of the monodansyl derivative **2** with 1,3-dibromobenzene, was unsuccessful.

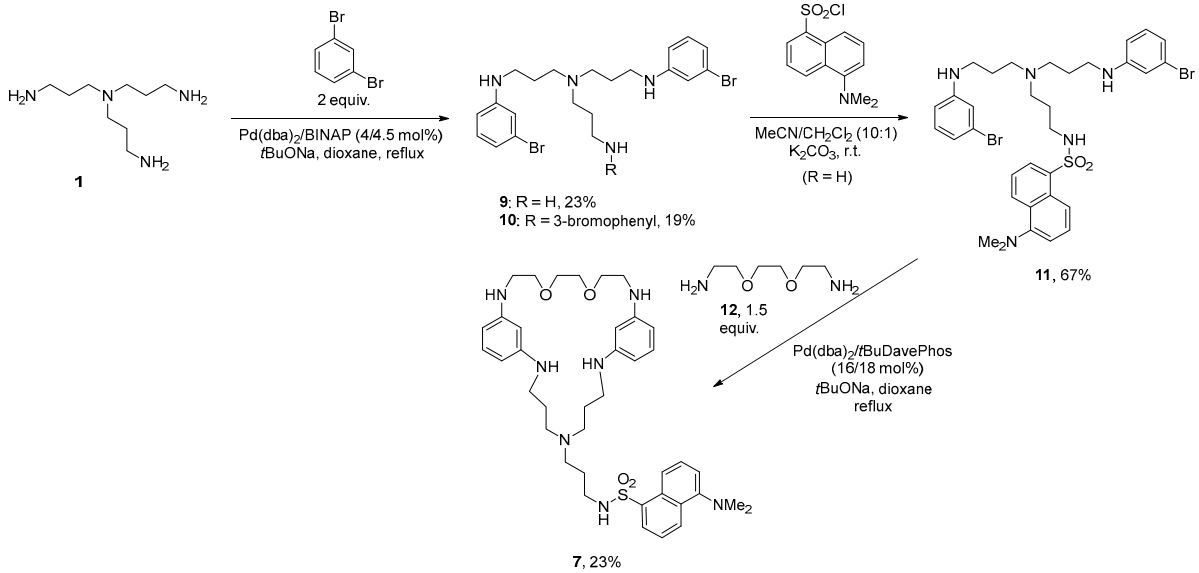

Scheme 3. Alternative synthesis of dansyl-substituted macrocycle 7.

The synthesis of the macrocycles comprising triamine and dioxadiamine chains and 6-quinolinyl substituents at the nitrogen atoms of the macrocycle was achieved according to Scheme 4. At the first step, the Pd-catalyzed heteroarylation of compound **7** with 6-bromoquinoline (3 equiv.) was carried out, which produced *N*,*N*′-di(quinolin-6-yl) derivative **13** in 34% yield, and the monoquinolinyl product **14** was isolated in 18% yield. The macrocyclization step employed the reaction with a branched tetraamine **1** (1.5 equiv.) and produced target macrocycles with two and one quinolinyl substituents **15** and **16**, respectively.

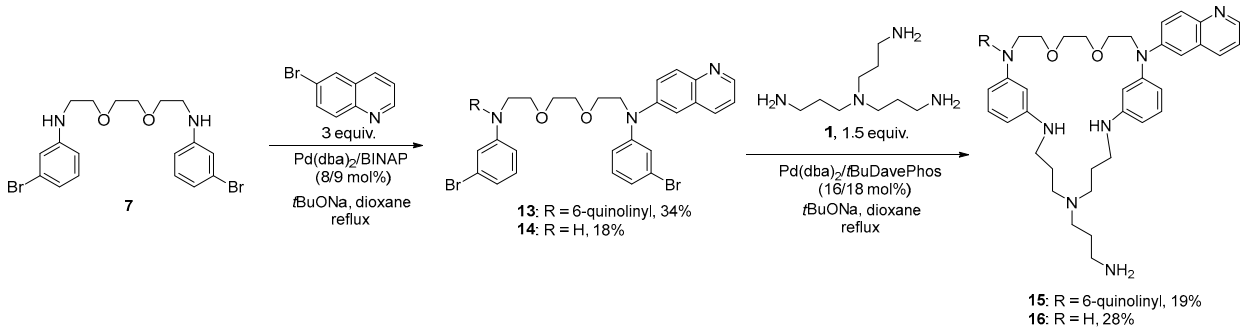

Scheme 4. Synthesis of di- and monoquinolinyl-substituted macrocycles 15 and 16.

To compare the binding properties towards various cations of the macrocycles with various sizes of the macrocyclic cavity, we synthesized several macrocycles starting from the *N*,*N*′-di(3-bromophenyl) derivative of trioxadiamine **17**, which possesses a longer chain (Scheme 5). We also were interested in the effect of the isomeric fluorophore group, i.e., 3-quinolinyl substituent, which could alter the binding abilities of the macrocycle due to a different orientation of the aromatic nitrogen with respect to a macrocyclic moiety. The compound **17** (which was obtained in accordance with the described method [34]) was reacted with three equiv. of either 6- or 3-bromoquinoline in the presence of $Pd(dba)_2$/BINAP (16/18 mol%). In both cases, di- and monoheteroarylated derivatives were obtained; moreover, the yields of the monoquinolinyl products **19** and **21** were somewhat higher than those of the diquinolinyl compounds **18** and **20**. This may be due to substantial hindrances in the formation of *N*,*N*,*N*′,*N*′-tetraaryl derivatives of di- and polyamines. Only the monoquinolinyl products **19** and **21** were further introduced in the macrocyclization reaction with the tetraamine **1**. Macrocycle **22** with 6-quinolinyl substituent was obtained in 17% yield, while its isomer **23** was synthesized in 28% yield.

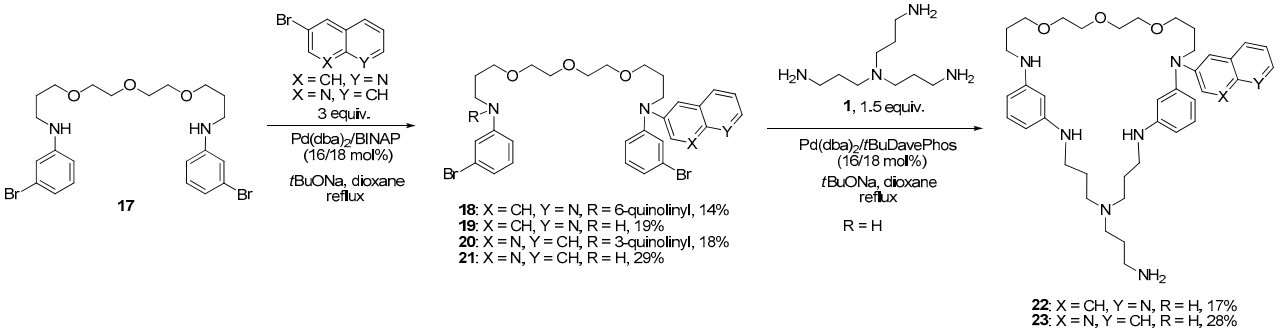

Scheme 5. Synthesis of monoquinolinyl-substituted macrocycles 22 and 23.

At last, the synthesis of the dansyl-substituted macrocycle with the triamine and trioxadiamine endocyclic chains was undertaken (Scheme 6). For this purpose, compound **17** was decorated with two dansyl groups forming intermediate product **24** in 70% yield, and afterwards, the macrocyclization reaction with the branched tetraamine **1** afforded the target macrocycle **25** in 26% yield. Thus, we have obtained a series of seven macrocycles

differing by the cavity size, type and position of fluorophore groups, which also possess additional donor sites that are able to participate in binding metal cations.

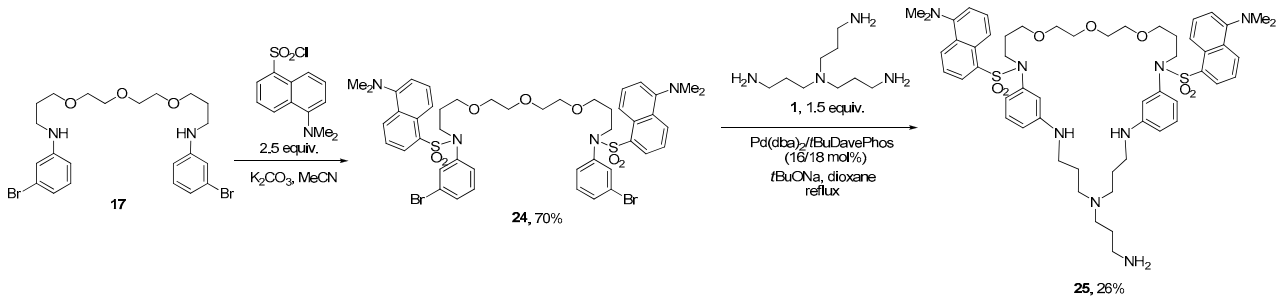

Scheme 6. Synthesis of didansyl-substituted macrocycle 24.

3.2. Spectroscopic Investigations

The investigation of the ability of the synthesized macrocycles to act as fluorescent detectors of metal cations was carried out using a panel of 21 salts: 18 perchlorates (Li(I), Na(I), K(I), Mg(II), Ca(II), Ba(II), Al(III), Cr(III), Mn(II), Fe(II), Co(II), Ni(II), Cu(II), Zn(II), Cd(II), Hg(II), Pb(II) and Ag(I)) and 3 nitrates (Ga(III), In(III) and Y(III)). The UV–vis and spectra of fluorescence were registered in MeCN, and the spectroscopic properties of the potential detectors **7**, **8**, **15**, **16**, **22**, **23** and **25** are presented in Table 1. Metal salt (perchlorate or nitrate) was added gradually to a ligand under investigation in the spectrofluorimetric cuvette (1, 2, 5, 10 equiv.), and upon each addition, the UV–vis and spectra of fluorescence were registered. For convenience, all figures present the data corresponding to five equiv. of metals salt added. In the case in which the changes in the spectrum caused by a certain ion were different from the changes observed with other metals, spectrophotometric and spectrofluorimetric titrations were conducted; in several cases, they were accompanied by the NMR titrations. As the macrocycles under investigation contain many *N*- and *O*-binding sites differing in their ability to form coordination bonds with metal cations, one may suppose that they will give complexes of different stabilities with various metals; moreover, complexes with different ligand-to-metal ratios can be formed with a certain cation, especially those characterized by a high coordination number. This will ensure different changes in absorption and fluorescence spectra that are crucial for the needs of detection.

Table 1. Spectroscopic properties of the macrocycles **7**, **8**, **16**, **22**, **23** and **25**.

Macrocycle	Concentration, μM	λ_{abs}, nm	lgε	λ_{ex}, nm	λ_{em}, nm
7	4.8	305	4.47	340	508
		340	4.20		
8	23.0	300	4.08	365	430
		365	3.66		
16	17.5	308	4.19	370	443
		373	3.80		
22	14.3	309	4.28	370	485
		374	3.86		
23	21.2	306	4.03	370	510
		370	3.68		
25	12.3	313	3.96	340	516
		342	3.93		

The addition of metal salts to the macrocycle **7** containing tris(3-aminopropyl)amine and dioxadiamine fragments and one dansyl group attached to an exocyclic amine caused either the quenching (Li(I), K(I), Cu(II), Hg(II)) or enhancement (other ions) of fluorescence—in some cases, with small bathochromic shifts in the emission maximum (by 10–15 nm) (Figure 1a). The changes in the absorption spectrum were not observed in the presence of the majority of cations, except for Cu(II), Hg(II) and Fe(III) (Figure S1). The addition of the copper perchlorate resulted in the disappearance of the absorption maximum at 310 nm, while in the presence of Hg(II) cations, two new, weakly manifested maxima at 315 and 350 nm emerged (Figure S2). As for $Fe(ClO_4)_3$, its addition simply caused an increase in the optical density of the specimen, which is likely due to the partial hydrolysis of this salt. The peculiarity of this salt, as well of $Mn(ClO_4)_2$, was also observed in further experiments and will not be discussed specially. In fact, macrocycle **7** did not show any selective response to the metal cations added and cannot serve for their detection.

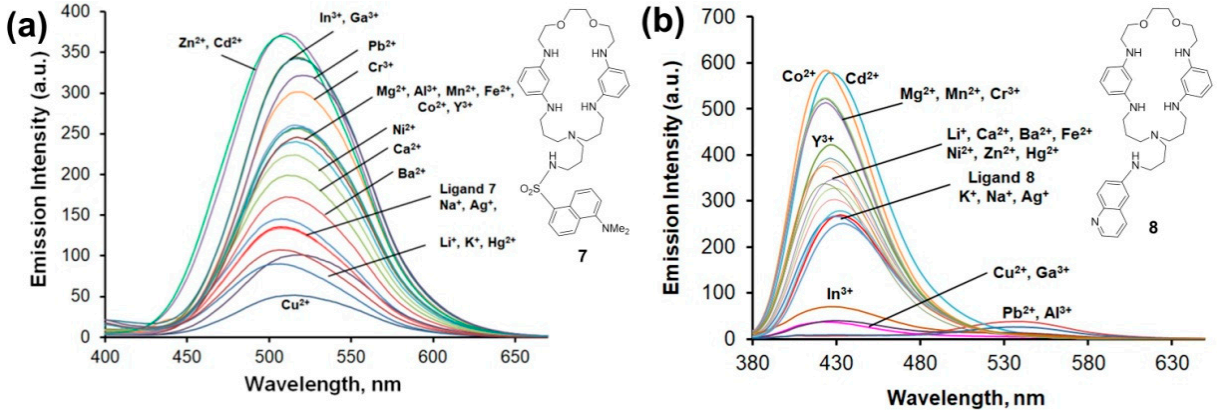

Figure 1. (**a**) Spectra of the fluorescence of compound **7** in the presence of Li(I), Na(I), K(I), Mg(II), Ca(II), Ba(II), Al(III), Cr(III), Mn(II), Fe(II), Co(II), Ni(II), Cu(II), Zn(II), Cd(II), Hg(II), Pb(II), Ag(I), Ga(III), In(III) and Y(III) (five equiv.). C_L 48 μM, λ_{ex} 340 nm. (**b**) Spectra of the fluorescence of compound **8** in the presence of Li(I), Na(I), K(I), Mg(II), Ca(II), Ba(II), Al(III), Cr(III), Mn(II), Fe(II), Co(II), Ni(II), Cu(II), Zn(II), Cd(II), Hg(II), Pb(II), Ag(I), Ga(III), In(III) and Y(III) (five equiv.). C_L 23 μM, λ_{ex} 365 nm.

The change in the dansyl fluorophore for the quinolin-6-yl substituent in the same compound fully changed the response of macrocycle **8** to the addition of the metal cations. In(III), Ga(III) and Cu(II) caused strong fluorescence quenching, while the addition of Al(III) and Pb(II) led to full emission quenching (Figure 1b). Moreover, in the presence of these cations, we observed a new emission band at *ca* 540 nm, which is only characteristic of these metals. Notable changes in the absorption spectrum were registered in the case of the following cations: Cu(II), Hg(II), Zn(II), Pb(II) and Al(III) (Figures S3 and S4). The addition of the copper perchlorate resulted in the disappearance of both absorption maxima at 300 and 365 nm; the same is true for $Hg(ClO_4)_2$, though in the case of Cu(II), the optical density increased throughout the whole spectrum. The changes caused by Zn(II) cations were less pronounced, but the addition of both Al(III) and Pb(II) salts gave rise to a new absorption band at 420 nm (Figure S4), while the initial maximum at 365 nm disappeared. The observed spectral changes allow for the proposal of macrocycle **8** as a potential dual-channel (colorimetric and fluorimetric) probe for Al(III) and Pb(II) cations as well as a colorimetric probe for Cu(II) cations.

The change in the position of the aminoquinolin-6-yl fluorophore group in the macrocycle in compound **16** (in which it is attached to an endocyclic nitrogen atom) leads to a dramatic change in the spectral response of the macrocycle to the presence of metal cations (Figure 2). The addition of some salts led to fluorescence quenching, while others promoted a moderate increase in the emission intensity, often with a small hypsochromic shift of

the maximum (*ca* 10 nm, like with Pb(II) or Mg(II)). The addition of Cd(II) caused both a bathochromic shift by 10 nm and some enhancement of fluorescence, while in the presence of Zn(II) perchlorate, this enhancement was much more pronounced (five times with five equiv.). In the UV–vis spectrum of **16** (Figures S5 and S6), it is clearly seen that the addition of Fe(III) and Mn(II) led to an increase in the optical density without changes in the shape (the probable reason is discussed above), the addition of Cu(II) ions resulted in a 10 nm hypsochromic shift of the maximum (from 370 to 360 nm). More interesting were the changes associated with the presence of Pb(II) and Al(III) cations, as they gave rise to a new absorption band at 440 nm. For this reason, we carried out spectrophotometric titration of the ligand with $Pb(ClO_4)_2$ (Figure S7) and calculated the binding constants for the L_4M, L_2M and LM complexes: lgβ = 17.5(3), lgβ = 10.27(1) and lgβ = 5.05(1), respectively. Figure S7b (absorption at 300 nm) shows that the local maximum corresponds to the L_4M complex, the local minimum of absorption corresponds to the L_2M composition and the formation of the LM complex brings the graph to a plateau. In Figure S7c, depicting the absorption at 440 nm, one may observe an increase in the absorption after the formation of the L_2M complex (0.5 equiv. Pb(II)). These data give evidence of a different coordination of lead cations at different titration steps. One may suppose that, at first, the coordination takes place at the aliphatic nitrogen atoms (NH_2 and NH), which lead to rather small changes in the absorption spectrum (calculated absorption spectra for L_4M and L_2M shown in Figure S8b), and more profound changes occur when the heterocyclic nitrogen from the quinoline moiety takes part in coordination with the Pb(II) cation, leading to a great bathochromic shift from 370 to 440 nm (calculated absorption spectrum for LM depicted in Figure S8b).

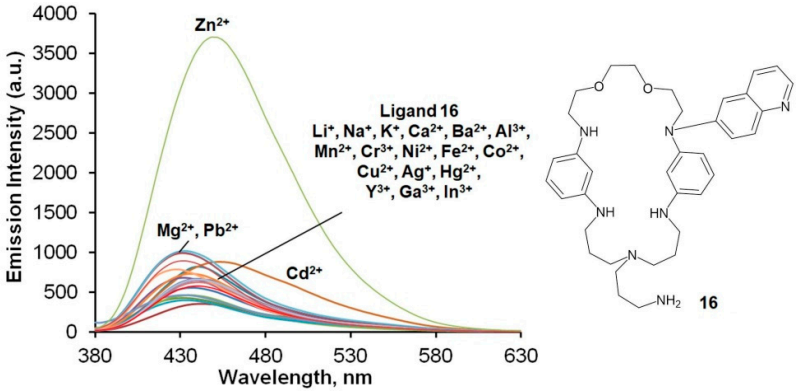

Figure 2. Spectra of the fluorescence of compound **16** in the presence of Li(I), Na(I), K(I), Mg(II), Ca(II), Ba(II), Al(III), Cr(III), Mn(II), Fe(II), Co(II), Ni(II), Cu(II), Zn(II), Cd(II), Hg(II), Pb(II), Ag(I), Ga(III), In(III) and Y(III) (five equiv.). C_L 17.5 μM, λ_{ex} 370 nm.

The attempt to proceed with the spectrofluorimetric titration of compound **16** with the Zn(II) perchlorate was unsuccessful, probably due to a partial oxidation of the diaminobenzene moiety in a dilute solution, but the changes in its UV–vis spectrum upon the addition of the same salt were helpful for obtaining data from its spectrophotometric titration (Figure S9a). The calculated binding constants for the L_2M, LM and LM_2 complexes are lgβ = 11.88(3), lgβ = 8.31(1) and lgβ = 12.2(3), respectively. Changes in the absorbance at 320 nm (Figure S9b) demonstrate a local minimum corresponding to the L_2M composition of the first complex, followed by a local maximum corresponding to the LM complex, but the changes in the absorbance intensity are quite small. The calculated UV–vis spectra (Figure S10a) show that it is the complex LM_2 that differs substantially from L, L_2M and LM by its spectrum, and it is characterized by a strong bathochromic shift of the absorption maximum from 370 to 440 nm (as was the case with Pb(II)). This suggests the participation of the fluorophore group (quinoline) in the coordination of the metal cation. However, the intensity of this new maximum is higher for the Pb(II) complex than for the Zn(II) complex.

The NMR titration of macrocycle **16** with the Zn(II) perchlorate provides additional information about a successive formation of complexes with different ligand-to-metal ratios (Figure 3). Though it is clearly seen that the signals broaden upon the addition of Zn(II) salt, especially in the aliphatic part of the spectrum (Figure 3a), one may follow the changes of the chemical shifts of the protons belonging to quinoline moiety. The formation of the L_2M complex is evidenced from the inflection at *ca* 0.5 equiv. Zn(II) for the H^{26} proton (Figure 3b) and the maximum at 0.5 equiv. Zn(II) for the H^{24} proton (Figure 4c). After the addition of one equiv. of the salt, the graphs approach the plateau. We tried to calculate the binding constants from NMR titration, but they were found to be much higher than the limit of this method ($lg\beta \leq 5$). Graphs of the changes in the chemical shifts as experimental and calculated points are given in Figure S29; they correspond to the formation of ML_2 and ML complexes.

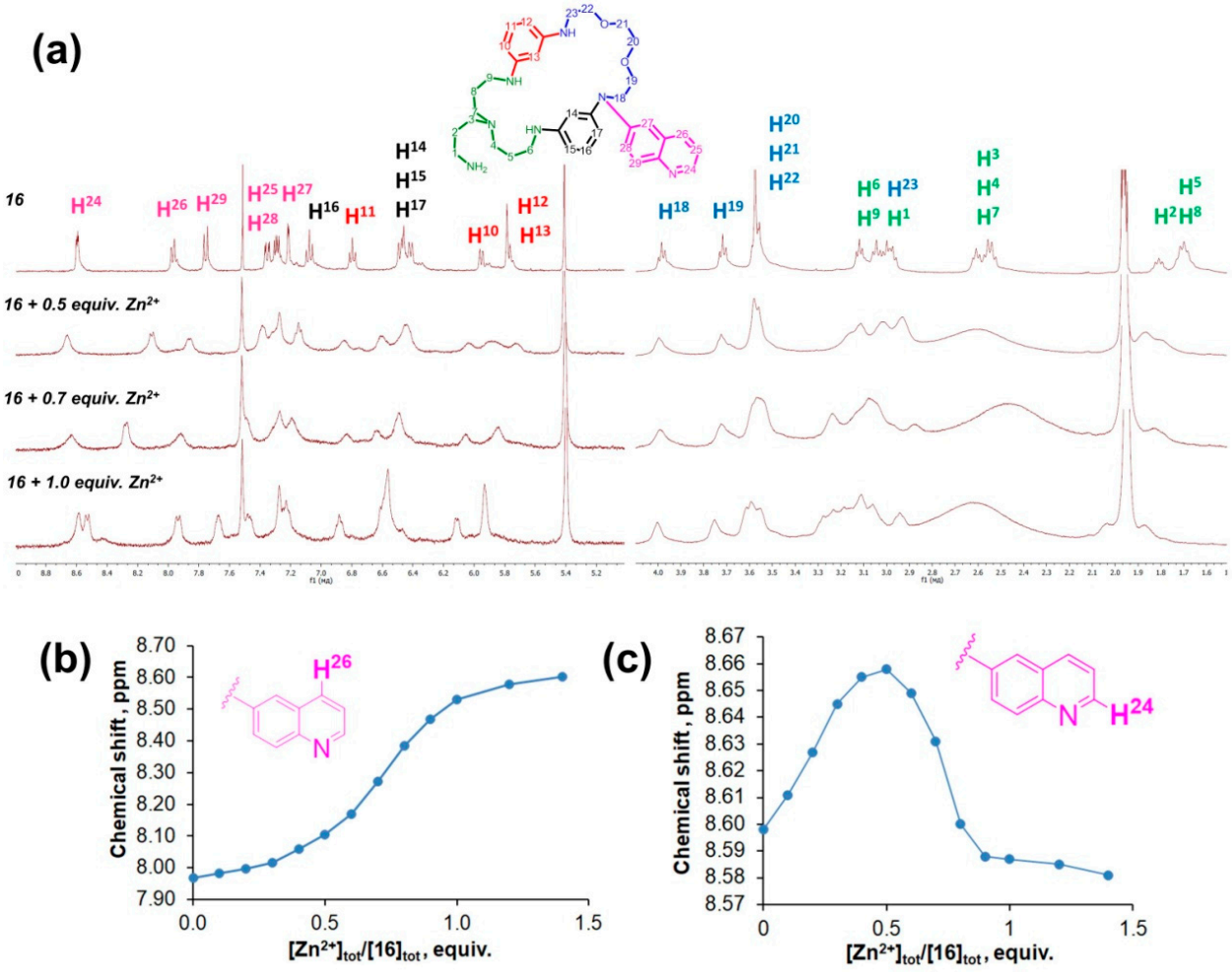

Figure 3. NMR titration of compound **16** with $Zn(ClO_4)_2{*}6H_2O$ in CD_3CN, C_L 0.041 M and $C_{Zn(II)}$ 0.2 M. (**a**) NMR spectra of **16** after the addition of 0.5, 0.7 and 1 equiv. of $Zn(ClO_4)_2$; (**b**) changes in the chemical shift of the H4(Quin) proton; (**c**) changes in the chemical shift of the H2(Quin) proton.

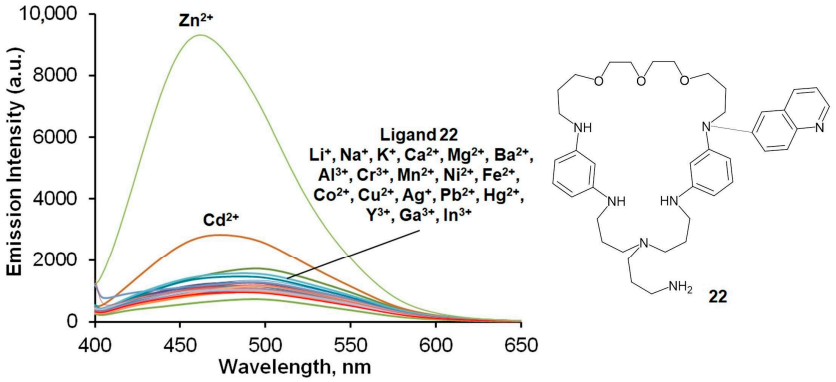

Figure 4. Spectra of the fluorescence of compound **22** in the presence of Li(I), Na(I), K(I), Mg(II), Ca(II), Ba(II), Al(III), Cr(III), Mn(II), Fe(II), Co(II), Ni(II), Cu(II), Zn(II), Cd(II), Hg(II), Pb(II), Ag(I), Ga(III), In(III) and Y(III) (five equiv.). C_L 14.3 μM, λ_{ex} 370 nm.

To conclude, macrocycle **16** can be judged as a potential fluorescent chemosensor for Zn(II) due to a described unique enhancement of emission in the presence of this cation, but its response in the UV–vis spectrum is quite similar for a number of cations and shows no selectivity.

Macrocycle **22** possesses a larger cavity compared to compound **16** due to the incorporation of the trioxadiamine structural unit instead of the dioxadiamine one. This unexpectedly resulted in a substantial red-shifted emission maximum (485 nm instead of 440 nm), but the general picture of the compound's response to the presence of the metal cations did not change dramatically (Figure 4). While the majority of metal salts caused either moderate fluorescence quenching or enhancement, only Cd(II) and, especially, Zn(II) led to a substantial increase in the emission intensity: the addition of five equiv. Cd(II) gave rise to 2.5-fold enhancement, and that of five equiv. Zn(II) resulted in a ninefold increase in the emission intensity. In both cases, a small hypsochromic shift of 10–15 nm was observed. The spectrofluorimetric titration of macrocycle **22** with $Zn(ClO_4)_2$ was successful (Figure S13) and revealed the formation of the complexes L_4M and L_2M with the corresponding binding constants lgβ = 28.2(1) and lgβ = 14.69(7). The calculated emission spectra (Figure S14a) demonstrate that the enhancement of the intensity of fluorescence is mainly associated with the L_2M complex. The qualitative limit of spectrofluorimetric detection for Zn(II) by compound **22** was estimated as 13 μM.

The changes in the UV–vis spectrum of ligand **22** in the presence of metal salts are shown in Figure S11. They are very close to those observed for its analog **16**, and certain changes can also be found upon the addition of Cu(II), Hg(II), Zn(II), Pb(II) and In(III); however, only in the presence of the Cu(II) and Hg(II) cations were reasonable changes in the shape of the absorption spectrum observed (Figure S12). In the case of Cu(II), the gradual addition of the salt led to a disappearance of the absorbance at 380 nm and the formation of a new maximum at 440 nm, which is clearly seen from the titration spectra (Figure S15a). The binding constants for the LM, LM_2 and LM_3 complexes were calculated to be lgβ = 8.45(8), lgβ = 16.1(1) and lgβ = 21.1(2). While the LM complex, according to its calculated absorption spectrum, possesses similar absorption maxima as the initial ligand **22**, the spectra of LM_2 and LM_3 are quite different and are characterized by the absorbance at 440 nm (Figure S16a). This may be explained by the fact that more than one copper cation can bind to a macrocycle with a big enough cavity comprising five nitrogen and three oxygen atoms and which additionally possesses the exocyclic 3-aminopropyl substituent and 6-quinolinyl moiety. It is plausible to suggest that, in the LM_2 and LM_3 complexes, the coordination of Cu(II) also takes place at the nitrogen atom of the fluorophore quinoline fragment, because, in these complexes, a strong bathochromic shift is observed. Macrocycle **22** can be proposed as a potential fluorescent chemosensor for Zn(II) ions.

In addition, the NMR titration of macrocycle **22** with $Cd(ClO_4)_2$ was carried out. The titration curve shown in Figure 5 for the H4(Quin) proton clearly shows the inflection at 0.5

equiv. of Cd(II) corresponding to the formation of the L_2M complex, and after the addition of one equiv. of the salt, the chemical shift comes to a plateau. The binding constants for the L_2M and LM complexes were calculated to be lgβ = 2.7(3) ± 0.31 and lgβ = 3.1(2) ± 0.24 by the EQNMR program. Graphs of the changes in the chemical shifts as experimental and calculated points are given in Figure S30.

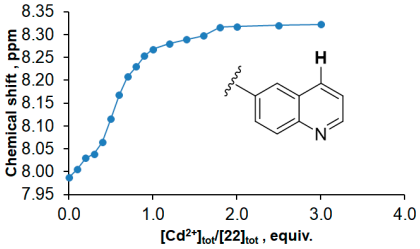

Figure 5. NMR titration of compound **22** with $Cd(ClO_4)_2{*}6H_2O$; changes in the chemical shift of the H4(Quin) proton. C_L 0.036 M, $C_{Cd(II)}$ 0.2 M.

Compound **23** possesses the same macrocyclic cavity as **22** decorated with the isomeric quinolin-3-yl fluorophore group. The fluorescence of this macrocycle is quenched to various degrees by the majority of the metal ions (Figure 6), but the addition of Cd(II) and, especially, Zn(II) salts leads to the enhancement of the emission intensity, with a notable hypsochromic shift of the maximum (by 15 and 30 nm, respectively). In the absorption spectra (Figure S17) of this compound in the presence of various metals, our attention was drawn to Zn(II) and Hg(II), as the changes caused by the addition of these metals were the most meaningful at the wavelength around 370 nm (the absorption maximum with the largest wavelength) (Figure S18). Spectrophotometric titration with $Zn(ClO_4)_2$ (Figure S19a) provided the binding constants lgβ = 21.34(5) for the Zn(II) complex of the L_4M composition and lgβ = 11.46(2) for the L_2M complex (Figure S20). Changes in the absorbance at 380 nm (Figure S19b) explicitly show the maximum at 0.25 equiv. of Zn(II), corresponding to the formation of the L_4M complex. The titration with $Hg(ClO_4)_2$ (Figure S21) revealed the formation of the following complexes: L_4M, L_2M, LM and LM_2. Their binding constants were calculated as lgβ = 22.94(8), lgβ = 13.23(7), lgβ = 7.80(5) and lgβ = 12.3(1), respectively (Figure S22). The changes in the UV–vis spectrum are complex, e.g., at 305 nm absorbance, it has a minimum at 0.25 equiv. of Hg(II) and a maximum at 1 equiv. of Hg(II), suggesting the formation of at least two complexes: L_4M and LM (Figure S21b). The calculated UV–vis spectra for different complexes show that these are LM and, especially, LM_2, which are characterized by the most important changes in the spectrum (Figure S22a). One may suggest that, with the ligand **23**, as in the above-described cases, at first, the most sterically accessible exocyclic NH_2 group can participate in binding with metal cations, giving rise to L_4M complexes, and further, upon the addition of more salt, the quinolinyl fluorophore group begins to take part in coordination, providing substantial changes in the absorption spectrum. It is even more plausible for the complexes with a metal-to-ligand ratio over 1. Thus, macrocycle **23** can be proposed as a dual-channel (UV and fluorescent) molecular probe for Zn(II) cations.

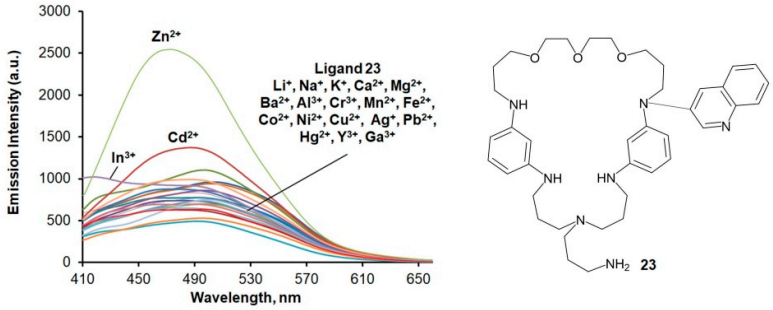

Figure 6. Spectra of the fluorescence of compound **23** in the presence of Li(I), Na(I), K(I), Mg(II), Ca(II), Ba(II), Al(III), Cr(III), Mn(II), Fe(II), Co(II), Ni(II), Cu(II), Zn(II), Cd(II), Hg(II), Pb(II), Ag(I), Ga(III), In(III) and Y(III) (five equiv.). C_L 21.2 μM, λ_{ex} 370 nm.

It was found that macrocycle **25**, featuring two dansyl fluorophore groups, exhibits a totally non-selective fluorescent response towards metal cations (Figure 7), like the above-described monodansyl macrocycle **7**. More distinguishable were the changes in its absorption spectrum upon the addition of several metal cations (Figure S23), including Zn(II) and Pb(II) (Figure S24). We carried out spectrophotometric titration with Zn(II) perchlorates (Figure S25). It was possible to calculate the binding constants for the L_4M and L_2M complexes with Zn(II) (lgβ = 25.3(1) and lgβ = 13.49(5)) (Figure S26). In the case of titration with $Pb(ClO_4)_2$ (Figure S27a), the absorbance in the interval of 310–340 nm first gradually increased up to 0.33 equiv. of Pb(II) and then began to diminish (Figure S27a,b). The calculation of the binding constants gave the following values for the L_3M, LM and LM_2 complexes: lgβ = 19.48(5), lgβ = 7.74(2) and lgβ = 12.1(1) (Figure S28). However, the overall changes in the UV spectra are small enough, and, thus, macrocycle **25** cannot serve for the colorimetric detection of cations.

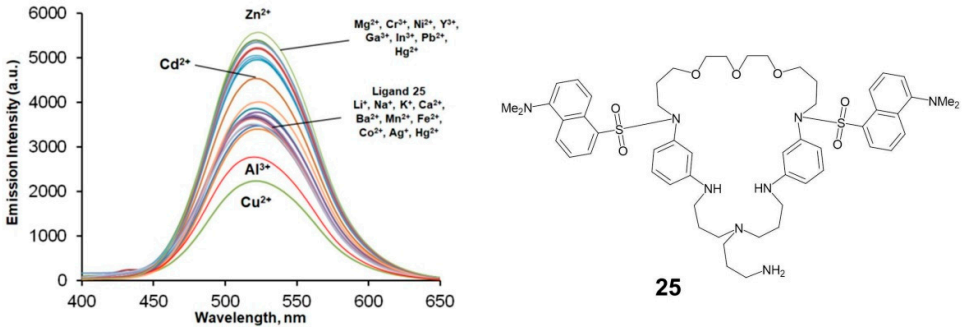

Figure 7. Spectra of the fluorescence of compound **25** in the presence of Li(I), Na(I), K(I), Mg(II), Ca(II), Ba(II), Al(III), Cr(III), Mn(II), Fe(II), Co(II), Ni(II), Cu(II), Zn(II), Cd(II), Hg(II), Pb(II), Ag(I), Ga(III), In(III) and Y(III) (five equiv.). C_L 12.3 μM, λ_{ex} 340 nm.

The NMR titration of macrocycle **25** with $Hg(ClO_4)_2$ was carried out as an alternative to spectrofluorimetric titration. The corresponding titration curve is shown in Figure 8 for the H4(Np) proton, and it features a maximum at 0.5 equiv. of Hg(II), corresponding to the formation of the L_2M complex. After this maximum, the chemical shifts gradually diminish but still do not approach the plateau at 1.5 equiv. of Hg(II) salt. The binding constants for the L_2M and LM complexes were calculated to be lgβ = 2.5(2) and lgβ = 3.8(2) by the BindFit program. Graphs of the changes in the chemical shifts as experimental and calculated points are given in Figure S31.

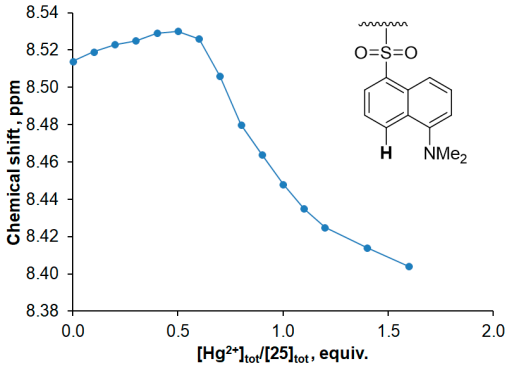

Figure 8. NMR titration of compound **25** with $Hg(ClO_4)_2{*}6H_2O$; changes in the chemical shift of the H4(Np) proton. C_L 0.046 M, $C_{Hg(II)}$ 0.2 M.

The data for the composition of the complexes and their binding constants are summarized in Table 2.

Table 2. Composition and binding constants for selected complexes of the macrocycles **16**, **22**, **23** and **25**.

Macrocycle	Metal	Complex	lgβ	Method
16	Pb(II)	L_4M	17.5(3)	Spectrophotometry
		L_2M	10.27(1)	Spectrophotometry
		LM	5.05(1)	Spectrophotometry
	Zn(II)	L_2M	11.88(3)	Spectrophotometry
		LM	8.31(1)	Spectrophotometry
		LM_2	12.2(3)	Spectrophotometry
22	Cu(II)	LM	8.45(8)	Spectrophotometry
		LM_2	16.1(1)	Spectrophotometry
		LM_3	21.1(2)	Spectrophotometry
	Zn(II)	L_4M	28.2(1)	Spectrofluorometry
		L_2M	14.69(7)	Spectrofluorometry
	Cd(II)	L_2M	2.7(3)	NMR (EQNMR)
		LM	3.1(2)	NMR (EQNMR)
23	Zn(II)	L_4M	21.34(5)	Spectrophotometry
		L_2M	11.46(2)	Spectrophotometry
	Hg(II)	L_4M	22.94(8)	Spectrophotometry
		L_2M	13.23(7)	Spectrophotometric
		LM	7.80(5)	Spectrophotometric
		LM_2	12.3(1)	Spectrophotometric
25	Zn(II)	L_4M	25.3(1)	Spectrophotometric
		L_2M	13.49(5)	Spectrophotometric
	Pb(II)	L_3M	19.48(5)	Spectrophotometric
		LM	7.74(2)	Spectrophotometric
		LM_2	12.1(1)	Spectrophotometric
	Hg(II)	L_2M	2.5(2)	NMR (BindFit)
		LM	3.8(2)	NMR (BindFit)

4. Conclusions

In this research, we elaborated a synthetic route to *N*- and O-containing macrocycles comprising the structural fragments of tris(3-aminopropyl)amine (TRPN) and dioxa- or trioxadiamines with additional fluorophore groups such as 5-(dimethylamino)naphthalene-1-sulfonyl (dansyl), 6- or 3-quinolinyl. First of all, macrocylization reactions were carried out under Pd(0)-catalyzed amination conditions. The possibility of introducing either free or *N*-(quinoline-6-yl)-substituted TRPN and *N*,*N*′-di(3-bromophenyl)-substituted oxadiamines bearing one or two additional fluorophore groups in the catalytic macrocyclization reactions was demonstrated. The synthesized macrocycles differ not only by the cavity size and nature of fluorophores but also by their position (attached either to exocyclic 3-aminopropyl fragments or to endocyclic nitrogen atoms). Six macrocycles were investigated for their ability to change their spectra of absorption and fluorescence in the presence of 21 metals. Among them, judging by a unique character of the changes in UV–vis and emission spectra, macrocycle **8**, bearing the 6-quinolinyl substituent at the exocyclic nitrogen atom, was shown to be a potential dual-channel (colorimetric and fluorimetric) probe for the Al(III) and Pb(II) cations as well as a colorimetric probe for Cu(II) cations. Isomeric macrocycle **16**, with the same fluorophore attached to an endocyclic nitrogen atom, can be judged as a potential fluorescent chemosensor for Zn(II) due to a unique enhancement of emission in the presence of this cation. Macrocycle **22**, with a larger cavity and 6-quinolinyl fluorophore substituent, can also be proposed as a potential fluorescent chemosensor for Zn(II) ions. Additionally, macrocycle **23**, bearing 3-quinolinyl fluorophore, is capable of dual-channel (UV and fluorescent) molecular sensing for Zn(II) cations. Dansyl-substituted macrocycles **7** and **25** did not show enough selectivity in their response towards metals. UV–vis and spectrofluorimetric titrations were carried out for the macrocyclic ligands **16**, **22**, **23** and **25**, and the composition of the complexes and binding constants were obtained for the Zn(II), Cu(II), Pb(II) and Hg(II) cations. It was shown that, in almost all cases, the formation of the complexes with a ligand-to-metal ratio over 1 takes place (L_4M, L_3M or L_2M complexes). The studied macrocycles possess several types of coordination sites: the primary amino group in the 3-aminopropyl arm, N and O atoms of the macrocycle, quinoline nitrogen or the dimethylamino group of the dansyl fluorophore. Taking this fact into consideration, one may explain the formation of the complexes of different stoichiometries. The coordination of the metal cation with the NH_2 group gives rise to ML_x complexes, the further addition of the metal salt leads to ML complexes in which the coordination with macrocycle heteroatoms is possible and an excess of metal salt favors the formation of M_xL complexes with the participation of the nitrogen atoms of the fluorophore groups. Such stepwise coordination is evidenced by UV and NMR spectra recorded over the course of titration experiments. Indeed, the calculated UV–vis spectra of the complexes suggest that profound changes in the spectra (strong bathochromic shifts of the absorption maxima) are associated with the complexes with smaller ligand-to-metal ratios (such as ML or ML_2). This is probably due to the initial coordination of the NH_2 group of the exocyclic substituent at a low metal concentration, followed by the involvement of the heterocyclic nitrogen atom of the fluorophore group in the coordination at higher concentrations of metal salts. The NMR titration of the compounds **16**, **22** and **25** with Zn(II), Cd(II) and Hg(II) perchlorates, respectively, gave additional information on the composition and binding constants of the corresponding complexes.

Supplementary Materials: The following supporting information can be downloaded at: https://www.mdpi.com/article/10.3390/chemosensors11030186/s1, Figures S1 and S2: UV–vis spectra for compound 7 in the presence of metal salts; Figures S3 and S4: UV–vis spectra for compound 8 in the presence of metal salts; Figures S5 and S6: UV–vis spectra for compound 16 in the presence of metal salts; Figures S7 and S8: UV–vis titration of compound 16 with Pb(ClO4)2; Figures S9 and S10: UV–vis titration of compound 16 with Zn(ClO4)2; Figures S11 and S12: UV–vis spectra for compound 22 in the presence of metal salts; Figures S13 and S14: UV–vis titration of compound 22 with Cu(ClO4)2; Figures S15 and S16: spectrofluorimetric titration of compound 22 with Zn(ClO4)2; Figures S17 and S18: UV–vis spectra for compound 23 in the presence of metal salts; Figures S19

and S20: UV–vis titration of compound 23 with Zn(ClO4)2; Figures S21 and S22: UV–vis titration of compound 23 with Hg(ClO4)2; Figures S23 and S24: UV–vis spectra for compound 25 in the presence of metal salts; Figures S25 and S26: UV–vis titration of compound 25 with Zn(ClO4)2; Figures S27 and S28: UV–vis titration of compound 25 with Pb(ClO4)2; Figures S29–S31: Graphs of the changes in the chemical shifts as experimental and calculated points.

Author Contributions: Conceptualization, A.D.A. and I.P.B.; methodology, A.D.A. and A.S.A.; investigation, D.S.K., N.M.C. and O.A.M.; visualization, A.S.A. and O.A.M.; writing—original draft preparation, D.S.K. and N.M.C.; writing—review and editing, A.D.A., A.S.A. and I.P.B.; supervision, I.P.B.; project administration, A.D.A.; funding acquisition, A.D.A. All authors have read and agreed to the published version of the manuscript.

Funding: This work was accomplished in the frames of the State contract of the chair of organic chemistry of the Moscow State University entitled "Synthesis and study of physical, chemical and biological properties of organic and organometallic compounds"—CITIC No-AAAAA-A; 21-121012290046-4.

Institutional Review Board Statement: Not applicable.

Informed Consent Statement: Not applicable.

Data Availability Statement: Not applicable.

Conflicts of Interest: The authors declare no conflict of interest.

References

1. Fantozzi, N.; Pétuya, R.; Insuasty, A.; Long, A.; Lefevre, S.; Schmitt, A.; Robert, V.; Dutasta, J.-P.; Baraille, I.; Guy, L.; et al. A new fluorescent hemicryptophane for acetylcholine recognition with an unusual recognition mode. *New J. Chem.* **2020**, *44*, 11853–11860.
2. Domínguez, M.; Blandez, J.F.; Lozano-Torres, B.; de la Torre, C.; Licchelli, M.; Mangano, C.; Amendola, V.; Sancenón, F.; Martínez-Máñez, R. A Nanoprobe based on gated mesoporous silica nanoparticles for the selective and sensitive detection of benzene metabolite t,t-muconic acid in urine. *Chem. Eur. J.* **2021**, *27*, 1306–1310. [PubMed]
3. Li, C.; Manick, A.D.; Dutasta, J.P.; Bugaut, X.; Chatelet, B.; Martinez, A. Frustrated behavior of Lewis/Brønsted pairs inside molecular cages. *Org. Chem. Front.* **2022**, *9*, 1826–1836.
4. Sarkar, S.; Sarkar, P.; Ghosh, P. Heteroditopic macrobicyclic molecular vessels for single step aerial oxidative transformation of primary alcohol appended cross azobenzenes. *J. Org. Chem.* **2021**, *86*, 6648–6664.
5. Li, C.; Manick, A.-D.; Jean, M.; Albalat, M.; Vanthuyne, N.; Dutasta, J.-P.; Bugaut, X.; Chatelet, B.; Martinez, A. Hemicryptophane cages with a C1-symmetric cyclotriveratrylene unit. *J. Org. Chem.* **2021**, *86*, 15055–15062. [CrossRef]
6. Paz Clares, M.; Aguilar, J.; Aucejo, R.; Lodeiro, C.; Albelda, M.T.; Pina, F.; Lima, J.C.; Parola, A.J.; Pina, J.; Seixas De Melo, J.; et al. Synthesis and H^+, Cu^{2+}, and Zn^{2+} coordination behavior of a bis(fluorophoric) bibrachial lariat aza-crown. *Inorg. Chem.* **2004**, *43*, 6114–6122.
7. Castillo, C.E.; Algarra, A.G.; Ferrer, A.; Angeles Máñez, M.; Basallote, M.G.; Paz Clares, M.; Soriano, C.; Teresa Albelda, M.; García-España, E. Equilibrium and kinetics studies on bibrachial lariat aza-crown/Cu(II) systems reveal different behavior associated with small changes in the structure. *Inorg. Chim. Acta* **2014**, *417*, 246–257.
8. Hamacek, J.; Elhabiri, M.; Le Guennic, B.; Shanzer, A.; Albrecht-Gary, A.-M. Metal-mediated interactions in homo- and hetero-bimetallic edifices with lanthanides: A study in solution. *Eur. J. Inorg. Chem.* **2022**, *2022*, e202200235.
9. Godart, E.; Long, A.; Rosas, R.; Lemercier, G.; Jean, M.; Leclerc, S.; Bouguet-Bonnet, S.; Godfrin, C.; Chapellet, L.L.; Dutasta, J.P.; et al. High-relaxivity Gd(III)-hemicryptophane complex. *Org. Lett.* **2019**, *21*, 1999–2003.
10. Johnston, H.M.; Freire, D.M.; Mantsorov, C.; Jamison, N.; Green, K.N. Manganese (III/IV) μ-oxo dimers and manganese (III) monomers with tetraaza macrocyclic ligands and historically relevant open-chain ligands. *Eur. J. Inorg. Chem.* **2022**, *2022*, e202200039. [CrossRef]
11. Massoud, S.S.; Mautner, F.A.; Vicente, R.; Gallo, A.A.; Ducasse, E. Dinuclear and Polynuclear Bridged Azido–Nickel(II) Complexes: Synthesis, Structure Determination, and Magnetic Properties. *Eur. J. Inorg. Chem.* **2007**, *2007*, 1091–1102. [CrossRef]
12. Golbedaghi, R.; Moradi, S.; Salehzadeh, S.; Blackman, A.G. Some metal complexes of three new potentially heptadentate (N4O3) tripodal Schiff base ligands; synthesis, characterizatin and X-ray crystal structure of a novel eight coordinate Gd(III) complex. *J. Mol. Struct.* **2016**, *1108*, 727–734. [CrossRef]
13. Salehzadeh, S.; Golbedaghi, R.; Rakhtshah, J.; Adams, H. A new series of manganese(II) complexes of three fully condensed Schiff base ligands derived from some symmetrical and asymmetrical tripodal tetraamines and 2-pyridinecarboxyaldehyde. *J. Mol. Struct.* **2021**, *1245*, 130982. [CrossRef]
14. Salehzadeh, S.; Golbedaghi, R.; Adams, H. Nickel(II) complexes of two potentially heptadentate(N7) Tripodal Schiff-base ligands; X-ray crystal structure and theoretical studies. *J. Mol. Struct.* **2022**, *1247*, 131359. [CrossRef]

15. Emami Khansari, M.; Johnson, C.R.; Basaran, I.; Nafis, A.; Wang, J.; Leszczynski, J.; Hossain, M.A. Synthesis and anion binding studies of tris(3-aminopropyl)amine-based tripodal urea and thiourea receptors: Proton transfer-induced selectivity for hydrogen sulfate over sulfate. *RSC Adv.* **2015**, *5*, 17606–17614. [CrossRef] [PubMed]
16. Guillon, J.; Cohen, A.; Gueddouda, N.M.; Das, R.N.; Moreau, S.; Ronga, L.; Savrimoutou, S.; Basmaciyan, L.; Monnier, A.; Monget, M.; et al. Design, synthesis and antimalarial activity of novel bis{*N*-[(pyrrolo[1,2-a]quinoxalin-4-yl)benzyl]-3-aminopropyl}amine derivatives. *J. Enzyme Inhib. Med. Chem.* **2017**, *32*, 547–563. [CrossRef]
17. Guillon, J.; Cohen, A.; Das, R.N.; Boudot, C.; Gueddouda, N.M.; Moreau, S.; Ronga, L.; Savrimoutou, S.; Basmaciyan, L.; Tisnerat, C.; et al. Design, synthesis, and antiprotozoal evaluation of new 2,9-bis[(substituted-aminomethyl)phenyl]-1,10-phenanthroline derivatives. *Chem. Biol. Drug Des.* **2018**, *91*, 974–995.
18. Murugesan, K.; Jeyasingh, V.; Lakshminarayanan, S.; Narayanan, S.; Piramuthu, L. Traditional hydrogen bonding donors controlled colorimetric selective anion sensing in tripodal receptors: First-naked-eye detection of cyanide by a tripodal receptor via fluoride displacement assay. *Spectrochim. Acta Part A* **2019**, *223*, 117238. [CrossRef]
19. Jeyasingh, V.; Murugesan, K.; Lakshminarayanan, S.; Selvapalam, N.; Das, G.; Piramuthu, L. Selective colorimetric sensing and perfect linear recognition of azide: Formation of Cu-azide-Cu cascade complex within the cavity of cryptand. *Spectrochim. Acta Part A* **2020**, *240*, 118550. [CrossRef]
20. Jeyasingh, V.; Murugesan, K.; Lakshminarayanan, S.; Selvapalam, N.; Das, G.; Enoch, I.V.M.V.; Piramuthu, L. Most efficient tris(3-aminopropyl) amine based electron deficient tripodal receptor for azide. *J. Fluoresc.* **2020**, *30*, 291–300. [CrossRef]
21. Wang, H.; Yuan, Y.; Zhuo, Y.; Chai, Y.; Yuan, R. Self-enhanced electrochemiluminescence nanorods of tris(bipyridine) ruthenium(II) derivative and its sensing application for detection of *N*-Acetyl-β-D-glucosaminidase. *Anal. Chem.* **2016**, *88*, 2258–2265. [CrossRef] [PubMed]
22. Louka, F.R.; Haq, S.J.; Guidry, H.R.; Williams, B.R.; Henary, M.M.; Fischer, R.C.; Torvisco, A.; Massoud, S.S.; Mautner, F.A. Polynuclear and coordination polymers of copper(II) complexes assembled by flexible polyamines and bridging rigid N-heterocyclic multicarboxylates. *Inorg. Chim. Acta* **2020**, *500*, 119240. [CrossRef]
23. Chernikova, E.A.; Glukhov, L.M.; Kustov, L.M.; Krasovsky, V.G. Adsorbents of SO_2 based on amine-modified porous materials. *Russ. Chem. Bull.* **2015**, *64*, 2958–2962. [CrossRef]
24. Lyu, H.; Li, H.; Hanikel, N.; Wang, K.; Yaghi, O.M. Covalent organic frameworks for carbon dioxide capture from air. *J. Am. Chem. Soc.* **2022**, *144*, 12989–12995. [CrossRef] [PubMed]
25. Hofmann, A.J.; Niederegger, L.; Hess, C.R. Neighbouring effects on catalytic epoxidation by Fe-cyclam in M2-PDIxCy complexes. *Dalton Trans.* **2020**, *49*, 17642–17648. [CrossRef]
26. Medina-Molner, A.; Rohner, M.; Pandiarajan, D.; Spingler, B. Mono- and dinuclear metal complexes containing the 1,5,9-triazacyclododecane ([12]aneN3) unit and their interaction with DNA. *Dalton Trans.* **2015**, *44*, 3664–3672. [CrossRef]
27. Chand, D.K.; Bharadwaj, P.K. Heteroditopic cryptands of tunable cavity size: Imposition of distorted geometry onto copper(II) and nickel(II) and molecular recognition of water molecules. *Inorg. Chem.* **1998**, *37*, 5050–5055. [CrossRef]
28. Krzystof, E.; Bordunov, A.V.; Bradshow, J.S. Synthesis of hexaazacryptands containing furan and benzene groups in the bridging arms. *J. Heterocycl. Chem.* **1998**, *35*, 169–171.
29. Yoon, J.; Ohler, N.E.; Vance, D.H.; Aumiller, W.D.; Czarnik, A.W. A fluorescent chemosensor signalling only Hg(II) and Cu(II) in water. *Tetrahedron Lett.* **1997**, *38*, 3845–3848. [CrossRef]
30. Beletskaya, I.P.; Averin, A.D.; Bessmertnykh, A.G.; Denat, F.; Guilard, R. Palladium-catalyzed amination in the synthesis of polyazamacrocycles. *Russ. J. Org. Chem.* **2010**, *46*, 946–967. [CrossRef]
31. Averin, A.D.; Beletskaya, I.P. Synthesis of polymacrocyclic compounds via Pd-catalyzed amination and evaluation of their derivatives as metal detectors. *Pure Appl. Chem.* **2019**, *91*, 633–651. [CrossRef]
32. Averin, A.D.; Grigorova, O.K.; Malysheva, A.S.; Shaferov, A.V.; Beletskaya, I.P. Pd(0)-catalyzed amination in the synthesis of chiral derivatives of BINAM and their evaluation as fluorescent enantioselective detectors. *Pure Appl. Chem.* **2020**, *92*, 1367–1386. [CrossRef]
33. Ukai, T.; Kawazura, H.; Ishii, Y.; Bonnet, J.J.; Ibers, J.A. Chemistry of dibenzylideneacetone-palladium(0) complexes: I. Novel tris(dibenzylideneacetone)dipalladium(solvent) complexes and their reactions with quinones. *J. Organomet. Chem.* **1974**, *65*, 253–266. [CrossRef]
34. Averin, A.D.; Shukhaev, A.V.; Golub, S.L.; Buryak, A.K.; Beletskaya, I.P. Palladium-catalyzed amination in the synthesis of polyazamacrocycles containing a 1,3-disubstiituted benzene moiety. *Synthesis* **2007**, *2007*, 2995–3012. [CrossRef]
35. Gans, P.; Sabatini, A.; Vacca, A. Investigation of equilibria in solution. Determination of equilibrium constants with the HYPERQUAD suite of programs. *Talanta* **1996**, *43*, 1739–1753. [CrossRef]
36. Hynes, M.J. EQNMR: A Computer program for the calculation of stability constants from nuclear magnetic resonance chemical shift data. *J. Chem. Soc. Dalton Trans.* **1993**, *1993*, 311–312. [CrossRef]
37. Thordarson, P. Determining association constants from titration experiments in supramolecular chemistry. *Chem. Soc. Rev.* **2011**, *40*, 1305–1323. [CrossRef]